

Stability and evolution of electromagnetic solitons in relativistic degenerate laser plasmas

Sima Roy^{1,*} and A. P. Misra^{1,†}

¹*Department of Mathematics, Siksha Bhavana, Visva-Bharati (A Central University), Santiniketan-731 235, India*

(Dated: 28 Oct 2020)

The dynamical behaviors of electromagnetic (EM) solitons formed due to nonlinear interaction of linearly polarized intense laser light and relativistic degenerate plasmas are studied. In the slow motion approximation of relativistic dynamics, the evolution of weakly nonlinear EM envelope is described by the generalized nonlinear Schrödinger (GNLS) equation with local and nonlocal nonlinearities. Using the Vakhitov-Kolokolov criteria, the stability of an EM soliton solution of the GNLS equation is studied. Different stable and unstable regions are demonstrated with the effects of soliton velocity, soliton eigenfrequency, as well as the degeneracy parameter $R = p_{Fe}/m_e c$, where p_{Fe} is the Fermi momentum and m_e the electron mass, and c is the speed of light in vacuum. It is found that the stability region shifts to an unstable one and is significantly reduced as one enters from the regimes of weakly relativistic ($R \ll 1$) to ultrarelativistic ($R \gg 1$) degeneracy of electrons. The analytically predicted results are in good agreement with the simulation results of the GNLS equation. It is shown that the standing EM soliton solutions are stable. However, the moving solitons can be stable or unstable depending on the values of soliton velocity, the eigenfrequency or the degeneracy parameter. The latter with strong degeneracy ($R > 1$) can eventually lead to soliton collapse.

I. INTRODUCTION

Extensive studies on the formation and dynamics of solitons has been receiving renewed interests because of their fundamental importance in nonlinear sciences, as well as an important candidate for the emergence of turbulence in nonlinear dispersive media (See, e.g., Ref. 1 and references therein). Highly relativistic degenerate dense plasmas are believed to exist in compact astrophysical objects, e.g., in the interior of white dwarfs, neutron star and magnetars with particle number density ranging from 10^{26} cm^{-3} to 10^{34} cm^{-3} . Such high-density degenerate plasmas may be directly created via ultraviolet or x-ray free electron lasers [2]. Also, by varying the laser intensity, partially or fully degenerate plasmas can also be produced in the laboratory [3], which makes laser produced plasmas to be useful recreating astrophysical plasmas in the laboratory. Thus, successful operations of lasers in laboratories open up new possibilities to study the EM pulse penetration and to explore the subsequent nonlinear dynamics in degenerate dense plasmas under laboratory conditions.

Recent investigations stipulate that currently available laser intensity is as high as above 10^{24} W/cm^2 [4]. In the laser-plasma interactions, the electrons (and also protons) at these high intensities may no longer be nonrelativistic but are forced to accelerate with velocities close to the speed of light in vacuum. Relativistic motion of these plasma particles strongly affects the dynamics of laser pulse propagation, especially when nonlinear effects, e.g., ponderomotive force come into the picture, and thereby

leading to various interesting nonlinear phenomena including the formation of relativistic EM solitons. The latter are localized structures associated with the density depletion of electrons in the ponderomotive force field of an intense laser beam of light. These solitons are usually formed behind the laser pulse and they propagate in the form of an envelope carrying a large part of the laser pulse energy and thereby serving as a candidate for laser beam energy conversion.

The nonlinear propagation EM solitons in different plasma environments has been investigated by a number of authors [5–8]. Furthermore, the dynamics of EM solitons in relativistic plasmas in an idealized case of circular polarization has been extensively studied within the framework of one-dimensional relativistic fluid model and particle-in-cell (PIC) simulations [9–12]. The theory has been revisited in the context of linearly polarized EM waves as well [13–15]. Recently, the formation of standing EM solitons for circularly polarized EM waves in degenerate relativistic plasmas has been studied by Mikaberidze *et al.* [11]. They showed that EM solitons can be stable both in weakly relativistic and ultrarelativistic degenerate plasmas. However, the existence and the stability of moving EM solitons in the context of linearly polarized intense laser in relativistic degenerate plasmas has not been explored in details.

In this paper, our aim is to study the dynamics of EM solitons that are formed due to the nonlinear interaction of linearly polarized intense laser beam of light and electron density perturbations driven by the laser ponderomotive force in relativistic degenerate dense plasmas. We show that the existence and stability of EM solitons are significantly modified by the effects of electron degeneracy. The analytical results are also shown to be in good agreement with the numerical simulation of the nonlinear evolution equation.

* simaroy031994@gmail.com

† apmisra@visva-bharati.ac.in; apmisra@gmail.com

II. DYNAMICAL EQUATIONS

The nonlinear interaction of linearly polarized finite amplitude intense laser pulse with longitudinal electron density perturbations that are driven by the laser ponderomotive force in a relativistic degenerate plasma can be described by the following set of dimensionless equations which are the EM wave equation, the electron continuity and momentum equations and the Poisson equation in the Coulomb gauge [15–17].

$$\left(\frac{\partial^2}{\partial t^2} - c^2 \frac{\partial^2}{\partial z^2}\right) A_x = \frac{\omega_{pe}^2 m_e c^2}{n_0 H_e} n_e^2 A_x, \quad (1)$$

$$\frac{\partial(\gamma_e n_e)}{\partial t} + \frac{\partial}{\partial z}(\gamma_e n_e v_{ez}) = 0, \quad (2)$$

$$\frac{d}{dt} \left(\frac{\gamma_e H_e v_{ez}}{n_e c^2} \right) = e \left(\frac{\partial \phi}{\partial z} - \frac{1}{2} \frac{e n_e}{\gamma_e H_e} \frac{\partial A_x^2}{\partial z} \right) - \frac{1}{\gamma_e n_e} \frac{\partial P_e}{\partial z}, \quad (3)$$

$$\frac{\partial^2 \phi}{\partial z^2} = 4\pi e(\gamma_e n_e - n_0), \quad (4)$$

where $d/dt \equiv \partial/\partial t + \mathbf{v}_j \cdot \nabla$, and e , n_e (with its equilibrium value n_0 in laboratory frame), m_e and v_{ez} are, respectively, the charge, the number density, the mass and z -component of the velocity of electrons. Since ions form the neutralizing background, $\gamma_i = 1$ and so, $\gamma_i n_i = n_0$, the equilibrium number density of electrons and ions. Thus, the electron number density in the Laboratory frame with its equilibrium and perturbation parts may be written as $n_L \equiv \gamma_e n_e = n_0 + n'_L$. Furthermore, c is the speed of light in vacuum, ω_{pe} is the electron plasma frequency, A_x is the x -component of the vector potential, ϕ is the electrostatic potential, P_e is the electron degeneracy pressure at zero temperature, given by, [18]

$$(P_e, \mathcal{E}_e) = \frac{m_e^4 c^5}{3\pi^2 \hbar^3} \left[f(R), R^3 (1 + R^2)^{1/2} - f(R) \right], \quad (5)$$

$$f(R) = \frac{1}{8} \left[R (2R^2 - 3) (1 + R^2)^{1/2} + 3 \sinh^{-1} R \right],$$

where $\hbar = h/2\pi$ is the reduced Planck's constant, $R = p_{Fe}/m_e c = \hbar (3\pi^2 n_e)^{1/3} / m_e c$ is the dimensionless degeneracy parameter, and $H_e \equiv P_e + \mathcal{E}_e = n_e m_e c^2 \sqrt{1 + R^2}$ is the enthalpy per unit volume measured in the rest frame of each element of the fluid with \mathcal{E}_e denoting the total energy density, i.e., $\mathcal{E}_e = m_e n_e c^2 + \bar{\epsilon}_e$ and $\bar{\epsilon}_e$ the internal energy of the fluid. Also, γ_e is the relativistic factor, given by, [17]

$$\gamma_e = \sqrt{\frac{1 + e^2 n_e^2 A_x^2 / H_e^2}{1 - v_{ez}^2 / c^2}}. \quad (6)$$

For the slow-motion approximation of relativistic dynamics of electrons, i.e., $e n_e A_x / H_e \sim o(\epsilon)$; ϕ , n_{e1} , $v_{ez} \sim$

$o(\epsilon^2)$, where $0 < \epsilon < 1$ is a scaling parameter, Eqs. (1) to (4) can be reduced to the following coupled equations [17].

$$\left(\frac{\partial^2}{\partial t^2} - \frac{\partial^2}{\partial z^2} + 1\right) A + (1 - \delta_e)(N - \alpha A^2)A = 0, \quad (7)$$

$$\left(\frac{\partial^2}{\partial t^2} - \delta_e \frac{\partial^2}{\partial z^2} + 1\right) N = \frac{1}{2}(1 - \delta_e) \frac{\partial^2 A^2}{\partial z^2}, \quad (8)$$

where $N \equiv N_{e1}/n_0 = \gamma_e n_e/n_0 - 1$ is the dimensionless longitudinal electron density perturbation and $A \equiv \eta_e e A_x / m_e c^2$ is the dimensionless vector potential along the x -axis. The space and time coordinates are normalized according to $t \rightarrow t\sqrt{\eta_e \omega_p}$, $z \rightarrow z\sqrt{\eta_e \omega_p}/c$. Also, $\alpha = \eta_e^2/2$, $\delta_e = (1 - \eta_e^2)/3$ and $\eta_e = 1/\sqrt{1 + R_0^2}$ with $R_0 = \hbar(3\pi^2 n_0)^{1/3}/mc$ denoting a measure of the strength of plasma degeneracy, i.e., $R_0 \ll 1$ corresponds to the weakly relativistic degenerate plasma, whereas $R_0 \gg 1$ is referred to as ultra-relativistic degenerate plasmas.

For the evolution and stability of EM solitons in relativistic degenerate plasmas, it appears much more difficult to solve the fully relativistic one-dimensional fluid model due to the generation of higher harmonics of linearly polarized incident laser pulse. However, a more convenient approach is to study the coupled equations (7) and (8) instead. So, we introduce a slowly varying complex wave envelope in the form. Here, we note that in contrast to circular polarization, the linearly polarized EM waves have odd harmonics for the vector potential A and even harmonics for the electron density perturbation N . Thus, we have

$$A = \frac{1}{2} (a e^{-it} + a^* e^{it}), \quad (9)$$

$$N = N_0 + \frac{1}{2} (N_2 e^{-i2t} + N_2^* e^{i2t}),$$

where the asterisk denotes the complex conjugate of the corresponding physical quantity. Substituting the expansions in Eq. (9) for A and N into Eq. (8), and collecting the zeroth and second harmonic terms ($\sim e^{-i2t}$), we obtain the following envelopes for N_0 and N_2 .

$$N_0 = \frac{1}{4}(1 - \delta_e)(|a|^2)_{zz}, \quad (10)$$

$$N_2 = -\frac{1}{12}(1 - \delta_e)(a^2)_{zz}.$$

Next, substituting Eq. (9) into Eq. (7), and collecting the first harmonic terms ($\sim e^{-it}$), we obtain the following equation for the EM wave amplitude a [For details see Appendix A.

$$i \frac{\partial a}{\partial t} + \frac{1}{2}(a)_{zz} + \frac{3}{8}\alpha(1 - \delta_e)|a|^2 a - \frac{1}{8}(1 - \delta_e)^2(|a|^2)_{zz} a$$

$$+ \frac{1}{48}(1 - \delta_e)^2(a^2)_{zz} a^* = 0. \quad (11)$$

Equation (11) has the form of a generalized nonlinear Schrödinger (GNLS) equation with local (cubic) as well as nonlocal (derivative) nonlinearities. It is noticed that both the cubic and nonlocal nonlinear coefficients are significantly modified by the effects of the relativistic electron degeneracy pressure. It is to be noted that in the limit of $R_0 \rightarrow 0$, Eqs. (10) and (11) assume the same form as Eqs. (7) and (8) in Ref. [14] after replacing A by a . However, there are some disagreements with the factor $1/2$ in the expression for N_2 [Eq. (10)] and in the last term of Eq. (11). This may be due to some sign mismatch in the coefficient of $(A^2/2)A$ [Eq. (7)] with the similar term in Ref. [14]. The cubic nonlinearity should be correctly as $(A^2/2)A$ or $(a^2/2)a$ instead of $-(a^2/2)a$ as in Ref. [14]. Similar nonlinear term with the correct positive sign can be found in some other previous investigations, e.g., Eq. (29) of Ref. [16].

We look for a localized stationary solution of Eq. (11) in the form of a moving soliton $a = \rho(\xi) \exp[i\theta(\xi) + i\lambda^2 t]$ where $\xi = z - v_0 t$ and v_0 is the soliton velocity in the moving frame of reference. Thus, substituting this solution into Eq. (11), we obtain the following equations for the soliton phase and the amplitude.

$$\begin{aligned} \theta_{\xi\xi}\rho \left[1 + \frac{1}{12}(1 - \delta_e)^2 \rho^2 \right] \\ + \theta_{\xi}\rho_{\xi} \left[2 + \frac{1}{3}(1 - \delta_e)^2 \rho^2 \right] - 2v_0\rho_{\xi} = 0, \end{aligned} \quad (12)$$

$$\begin{aligned} \rho_{\xi\xi} - \frac{5}{12}(1 - \delta_e)^2 \frac{\rho}{\zeta} \rho_{\xi}^2 = \frac{\rho}{\zeta} (2\lambda^2 - 2v_0\theta_{\xi} + \theta_{\xi}^2) \\ + \frac{\rho^3}{\zeta} \left[\frac{1}{6}(1 - \delta_e)^2 \theta_{\xi}^2 - \frac{3}{4}\alpha(1 - \delta_e) \right] = 0, \end{aligned} \quad (13)$$

where $\zeta(\rho) = 1 - (5/12)(1 - \delta_e)^2 \rho^2$. Using the same boundary conditions, namely $\rho, \rho_{\xi}, \rho_{\xi\xi} \rightarrow 0$ as $\xi \rightarrow \pm\infty$, the integration of Eq. (12) approximately yields $\theta(\xi)_{\xi} = v_0$, while that of Eq. (13) gives

$$\rho_{\xi}^2 = \frac{\rho^2}{\zeta} \left(2\lambda^2 - v_0^2 - \left[\frac{3}{8}\alpha(1 - \delta_e) - \frac{1}{12}(1 - \delta_e)^2 v_0^2 \right] \rho^2 \right). \quad (14)$$

Further integration of Eq. (14) yields a soliton solution in the following implicit form.

$$\begin{aligned} \pm\xi = \sqrt{\frac{10(1 - \delta_e)}{\Delta}} \ln \frac{\sqrt{\zeta} + \sqrt{\zeta - \zeta_0}}{\sqrt{|\zeta_0|}} \\ - \frac{1}{2\sqrt{2\lambda^2 - v_0^2}} \ln \frac{\sqrt{1 - \rho^2/\rho_0^2} + \sqrt{\zeta}}{\left| \sqrt{1 - \rho^2/\rho_0^2} - \sqrt{\zeta} \right|}, \end{aligned} \quad (15)$$

where $\zeta_0(\rho_0) = 1 - (5/12)(1 - \delta_e)^2 \rho_0^2$, $\Delta = 9\alpha - 2(1 - \delta_e)v_0^2$ and

$$\rho_0^2 = \frac{24(2\lambda^2 - v_0^2)}{\Delta(1 - \delta_e)} \quad (16)$$

is the squared amplitude (maximum) of the linearly polarized moving EM soliton with the reduced eigenfrequency $\Lambda \equiv \lambda^2 - v_0^2$. In particular, for $v_0 = 0$, one can obtain the standing soliton solution of the GNLS equation (11). In general, Eq. (15) describes a two-parameter family of solutions of Eq. (11) which are symmetric about the origin, and while combined together generates the form a soliton. As an illustration, we plot the soliton solution [Eq. (15)] as shown in Fig. 1 for different values of the parameters v_0, λ and R_0 . It is seen that for a fixed value of R_0 and λ but with an increasing value of the soliton velocity, the amplitude decreases while the soliton profile (width) broadens. An opposite feature is observed with increasing value of λ , i.e., the soliton amplitude increases but the width decreases. However, when the relativistic degeneracy effect is more pronounced, an enhancement of both the amplitude and width of the soliton is seen to occur. In order to justify the physics behind it we consider the the small amplitude limit of solitons in which the nonlocal (ponderomotive) nonlinear terms may be neglected so that one recovers the cubic NLS equation from Eq. (11) as

$$i\frac{\partial a}{\partial t} + P\frac{\partial^2 a}{\partial z^2} + Q|a|^2 a = 0, \quad (17)$$

where $P = 1/2$ and $Q = (3/8)\alpha(1 - \delta_e)$. Equation (17) has a traveling wave solution of the form $a \sim \sqrt{a_0} \operatorname{sech}[(z - v_0 t)/w]$, where $wa_0 = \sqrt{2|P/Q|}$. Physically, the relativistic degeneracy pressure of electrons provides the wave dispersion (which increases with increasing values of R_0) quite distinctive from the dispersion due to separation of charged particles. So, depending on the dispersion and nonlinear effects, the soliton amplitude and width can increase or decrease. Since P appears as a constant due to its normalization, the wave amplitude/width can increase or decrease according to when the value of the nonlinear coefficient Q decreases or increases. It is noted that the values of Q decrease with increasing values of R_0 . Thus, it may be likely that the soliton amplitude and width can increase with increasing values of R_0 . However, when the wave amplitude is not small, the ponderomotive nonlinear effects can intervene the dynamics and compete with the cubic nonlinearity which may result into an increase of the wave amplitude and/or width or some other nonlinear phenomena including collapse.

III. STABILITY ANALYSIS

In order to examine the stability of the moving EM soliton, we follow the Vakhitov-Kolokolov stability criteria [19]. According to the criteria, solitons are stable under the longitudinal perturbations if

$$\frac{dP_0}{d\lambda^2} > 0, \quad (18)$$

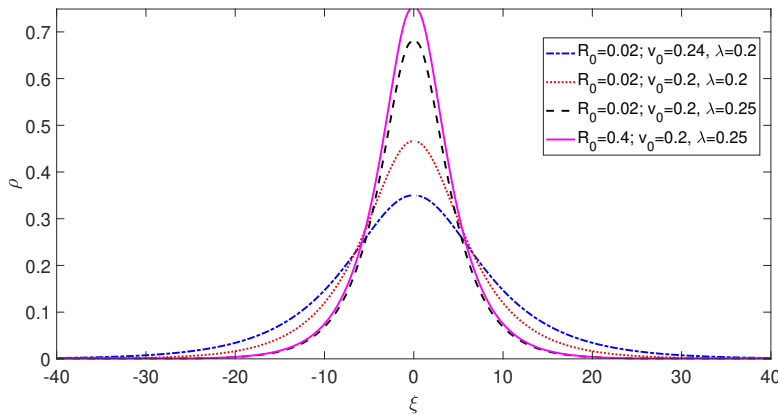


FIG. 1. A profile of the EM soliton, given by Eq (15), is shown for different values of the relativistic degeneracy parameter R_0 , the soliton eigenfrequency λ , and the soliton velocity v_0 as in the legend.

where P_0 is the soliton photon number defined by

$$P = \int |a|^2 dz. \quad (19)$$

An expression for $P_0(\lambda)$ can be obtained for the soliton solution (15) as

$$P_0(\lambda) = \frac{\sqrt{6}}{\sqrt{\Delta(1-\delta_e)}} \left(\rho_0 + \sqrt{\frac{3}{5}} \frac{\zeta_0}{1-\delta_e} \ln \frac{1+\sqrt{1-\zeta_0}}{|1-\sqrt{1-\zeta_0}|} \right) \quad (20)$$

So, according to the condition (18), the moving EM soliton (15) turns out to be stable in the region $\lambda < \lambda_s$, where λ_s is some instability threshold value of λ at which P_0 reaches a local maximum and above which $dP_0/d\lambda^2 < 0$. An analytic expression of λ_s cannot be determined in its explicit form. However, we try to find its values numerically for different values of the degeneracy parameter R_0 and the soliton velocity v_0 .

The profiles of the curves of $P_0(\lambda)$, as shown in Fig. 2, predicts the existence of stable ($\lambda < \lambda_s$) and unstable regions ($\lambda > \lambda_s$). It is found that an increase of the soliton velocity v_0 shifts the instability threshold λ_s towards larger values of it than that for the standing soliton with $v_0 = 0$ (see the solid and dashed curves). However, λ_s can shift towards its lower values if the degeneracy parameter R_0 is increased (see the dotted and dash-dotted curves). It follows that the stability domain $\lambda < \lambda_s$ of EM solitons may be significantly reduced in the regime of strongly or ultrarelativistic degenerate plasmas ($R_0 \gg 1$). We mention that the Vakhitov-Kolokolov criterion predicts only a linear stability of EM solitons involving the exponentially growing or decaying modes. So, it may not predict about the subsequent nonlinear evolution of unstable EM envelopes or about the stability of localized structures with arbitrary profiles. In general, the GNLS equation (11) can admit, apart from the stationary soliton solution, the soliton collapse [20] and long-lived relaxation oscillations around the stable soliton amplitude due

to cubic nonlinearity, and perhaps some other dynamical states due to the presence of nonlocal nonlinearities [14, 21]. An alternative stability criterion for the solitons can also be formulated in terms of the Hamiltonian and photon number interrelation (See, e.g., Ref. 13). We, however, skip this analysis here, instead look for some other regimes for the existence and stability of solitons by revisiting the Vakhitov-Kolokolov stability criterion and the constraints on the parameters λ and v_0 in the analytical soliton solution (15). The limits of λ and v_0 are given by

$$2\lambda^2 - v_0^2 > 0, \quad \zeta \equiv 1 - 5\rho^2(1-\delta_e)^2/12 > 0. \quad (21)$$

On more limitation on the parameter v_0 is given by

$$\Delta \equiv 9\alpha - 2(1-\delta_e)v_0^2 > 0, \quad \text{i.e., } v_0 < v_s \equiv \sqrt{9\alpha/2(1-\delta_e)}. \quad (22)$$

An estimation reveals that for $0 < (\alpha, \delta_e, v_0) < 1$, the condition $\Delta > 0$ holds for $0 \leq R_0 \lesssim 1.36$ and $\Delta < 0$ for $R > 1.36$.

In what follows, considering all the stability conditions, namely Eqs. (18), (21) and (22) imposed on the parameters λ and v_0 , we define the regions of the soliton existence and stability in (v_0, λ) -plane as shown in Fig. 3. We find that above the dashed curve of $\zeta \equiv 1 - 5\rho^2(1-\delta_e)^2/12 = 0$, no analytic soliton solution exists as the conditions are not satisfied there. However, one can obtain numerically a soliton solution of Eq. (11) there. Such a discrepancy in this particular region occurs due to an initial small phase $[\theta(\xi)]$ difference between these approximate analytical and numerical soliton solutions. Furthermore, below the solid curve of $2\lambda^2 - v^2 = 0$ no localized solution (analytical or numerical) can exist. The existence region of solitons is separated by a dotted curve. Between the dashed and the dotted curves is the region where $dP_0/d\lambda^2 < 0$, but both $2\lambda^2 - v^2$ and $\zeta > 0$, and so in this region only unstable soliton solution exists. However, the stable soliton region is in between the solid and dotted curves where all the conditions for soliton stability are satisfied. From the subplots (a) to (c)

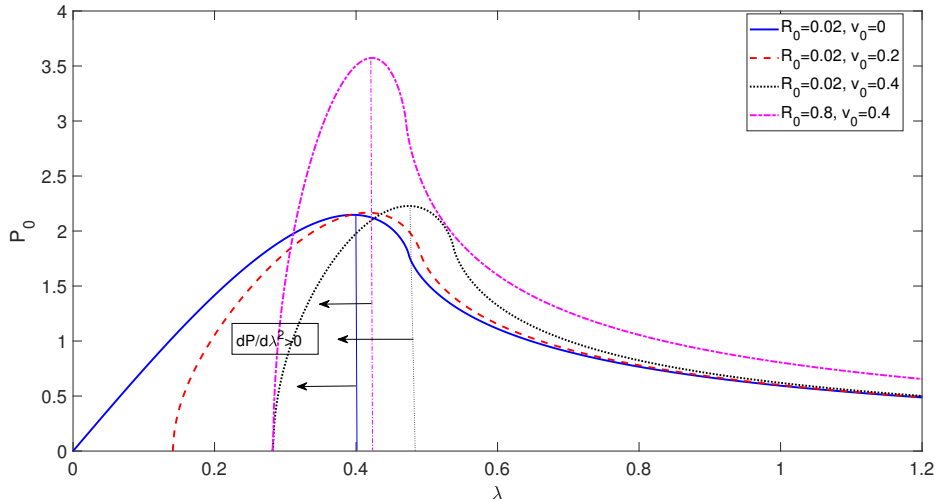


FIG. 2. Photon number $P_0(\lambda)$, given by Eq. (20), is plotted against the eigenfrequency λ to show the stable ($\lambda < \lambda_s$; $dP_0/d\lambda^2 > 0$) and unstable ($\lambda > \lambda_s$; $dP_0/d\lambda^2 < 0$) regions for different values of the relativistic degeneracy parameter R_0 and the soliton velocity v_0 as in the legend. The straight lines are drawn to indicate the corresponding threshold values λ_s of λ at which P_0 reaches a maximum value.

it is noticed that as we gradually enter from the regimes of weak, moderate to strong relativistic degenerate plasmas (by increasing the value of the degeneracy parameter R_0) both the stable and unstable regions get significantly compressed. Also, a stable region shifts to an unstable one as R_0 increases. Furthermore, subplot (c) shows that a threshold value v_s of v_0 appears when $R_0 > 1.36$. In fact, for $R_0 \gg 1$, no stable or unstable region may be found in the (v_0, λ) -plane. This may be the limitation of the linear stability analysis which may not correctly predict the existence and the stability regions of moving solitons, especially in the regime of ultrarelativistic degeneracy.

IV. SIMULATION RESULTS

So far we have obtained the possible regimes for the existence and stability of EM solitons based on an analytic stationary soliton solution of the GNLS equation (11). Next, we examine these regimes by a direct numerical simulation of Eq. (11). To this end, we use the Runge-Kutta scheme with a time step $dt = 0.001$ and with an initial condition in the form of a soliton: $a(\xi, 0) \sim a_0 \text{sech}^2(\xi/5) \exp(-iv_0\xi)$. The soliton evolution after time $t = 300$ is shown in Figs. 4 and 5 for different values of v_0 , λ and R_0 relevant for stable and unstable regions (*cf.* Fig. 3) as predicted in Sec. III. Here, we note that the initial condition may not be a solution to the GNLS equation (11). However, as time goes on, the initial pulse radiates and the nonlinear and dispersion effects intervene to evolve it as stable or unstable solitons. Numerical simulation reveals that initially launched soliton (15) with parameters v_0 , λ and R_0 in

the stable region remains stable for a long time. However, the stable or unstable behaviors may be changed if one considers the parameter values slightly above or below the stable or unstable region.

Figure 4 shows the evolution of EM solitons in the weakly relativistic regime ($R_0 = 0.02$). It is found that in the stable region, the standing soliton ($v_0 = 0$) with amplitude $a_0 = 0.68$, $\lambda = 0.207$ and photon number $P = 1.46$ oscillates around the stable equilibrium with a frequency close to the plasma oscillation frequency and so the soliton propagation remains stable for a long time [subplots (a) and (b)]. However, the moving soliton with the same $\lambda = 0.207$ but with an increased velocity $v_0 = 0.2$ and reduced amplitude $a_0 = 0.67$ in the stable region travels towards the downstream and exhibits decay of its amplitude [subplots (c) and (d)]. Physically, for a fixed λ , as the soliton velocity increases, its frequency of oscillation decreases. This results into a diminution of the photon number from $P = 1.46$ to $P = 1.12$, and thereby leading to a decay of the soliton amplitude. However, as time goes on it relaxes towards a corresponding stable soliton. On the other hand, retaining the soliton speed at $v_0 = 0.2$, but increasing its amplitude to $a_0 = 0.72$ and the frequency to $\lambda = 0.26$, we find that both the soliton eigenfrequency and the photon number ($P_0 = 1.55$) increase. As a result, though the soliton evolves with long-lived oscillating behaviors of the breather type, its amplitude grows and it may be prone to instability [subplots (e) and (f)]. A slight deviation from the stable equilibrium with an increase of λ or the initial perturbation with an increased amplitude a_0 for a fixed soliton velocity can lead to an aperiodic growth of the amplitude and thereby the onset of collapse.

In order to examine the effects of the relativistic de-

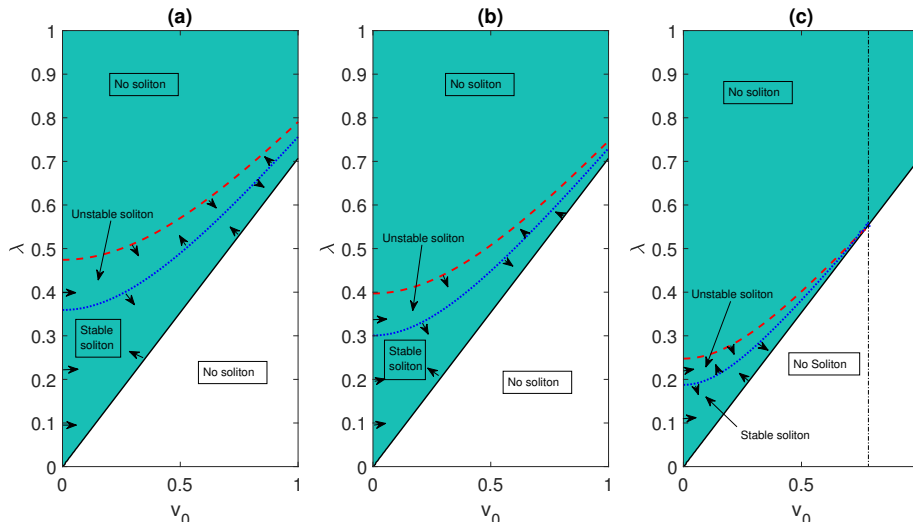


FIG. 3. The regions for the existence of EM solitons and their stability are shown in the (v_0, λ) -plane for different values of the relativistic degeneracy parameter R_0 : (a) $R_0 = 0.02$, (b) $R_0 = 0.8$ and (c) $R_0 = 2$. The solid, dashed and dotted lines, respectively, represent the contour plots of $2\lambda^2 - v^2 = 0$, $\zeta \equiv 1 - (5/12)\rho^2(1 - \delta_e)^2 = 0$ and $dP_0/d\lambda^2 = 0$. In the subplot (c), the dash-dotted line represents a threshold value of v_0 : $v_s = 0.78$ above which no soliton solution exists as $\Delta \equiv 9\alpha - 2(1 - \delta_e)v_0^2 < 0$ there. Note that the value of v_s decreases with increasing values of $R_0 > 1.36$. No such threshold exists in the region $0 \leq v_0 \leq 1$, $0 \leq \lambda \leq 1$ when R_0 lies in $0 \leq R_0 \lesssim 1.36$.

generacy on the soliton dynamics, we consider three different values of R_0 , namely $R_0 = 0.02$, $R_0 = 0.8$ and $R_0 = 2$ to define, respectively, the weak, moderate and strong degeneracy of electrons. With reference to Fig. 3 (which predicts that the soliton stable region can shift to an unstable one by an increasing value of R_0) we see from Fig. 5 that for some fixed values of $\lambda = 0.23$ and $v_0 = 0.2$, as R_0 increases the soliton amplitude grows, it loses its stability and eventually collapses. Subplots (a) and (b) show that in the weakly relativistic regime of electron degeneracy, a moving soliton with an amplitude $a_0 = 0.6$ in the stable region travels towards downstream with preserving its profile, i.e., the soliton remains stable for a longer time. The solitons also remain stable even in the limit of $R_0 \rightarrow 0$, i.e., when there is no electron degeneracy. If the initial soliton profile is considered with an increased amplitude with $a_0 = 0.82$ in the regime of moderate degeneracy with $R_0 = 0.8$, the soliton amplitude grows but it evolves about the stable equilibrium until it remains in the stable region [subplots (c) and (d)]. However, as the parameter R_0 is further increased to $R_0 = 2$, the moving soliton with amplitude $a_0 = 1.6$ falls in the unstable region. In this situation, solitons can not travel undistorted with a constant velocity. Its amplitude aperiodically grows and eventually collapses [subplots (e) and (f)].

We note that when the electron degeneracy effect is small, i.e., $R_0 \ll 1$, one finds $\eta_e \sim 1$ and $\delta_e \ll 1$ for which the coefficients of the GNLS equation (11) appear as constants. In this case, one recovers the similar results as in Ref. [14] with no degeneracy of electrons. However, for moderate or large values of R_0 , as the parameter in-

creases, the magnitudes of both the cubic and nonlocal nonlinearities tend to decrease, which results into an enhancement of the soliton amplitude and/or width. This is expected, since in absence of the nonlocal terms, the GNLS equation (11) admits a soliton solution with amplitude/width proportional to $\sqrt{|P/Q|}$, where P corresponds to the group velocity dispersion and Q the cubic nonlinear effects. However, in presence of the nonlocal nonlinearities, not only the solitons grow with higher values of R_0 , a rapid aperiodic growth in amplitude creates a collapsing soliton until the amplitude reaches a critical value, and we can no longer observe the dynamic behaviors. The subplot 5(e) shows that when the values of v_0 , and λ fall slightly outside the stable region [cf Fig. 3(c)], the soliton amplitude grows to become unstable, and eventually collapses. From the subplot 5(f), it may be estimated that the soliton collapse starts to occur after time $t \sim 160$, and within the time interval $0 < t < 160$, the soliton amplitude remains of the order of unity. Thus, our analytical predictions for the existence and stability of EM solitons agree with the numerical results that an increase of the soliton velocity shifts the instability threshold towards larger values, and the strong degeneracy effects can shift the steady state dynamics of solitons to an unstable one which results into wave collapse.

V. CONCLUSION

We have studied the stability and dynamical evolution of electromagnetic (EM) solitons that are formed

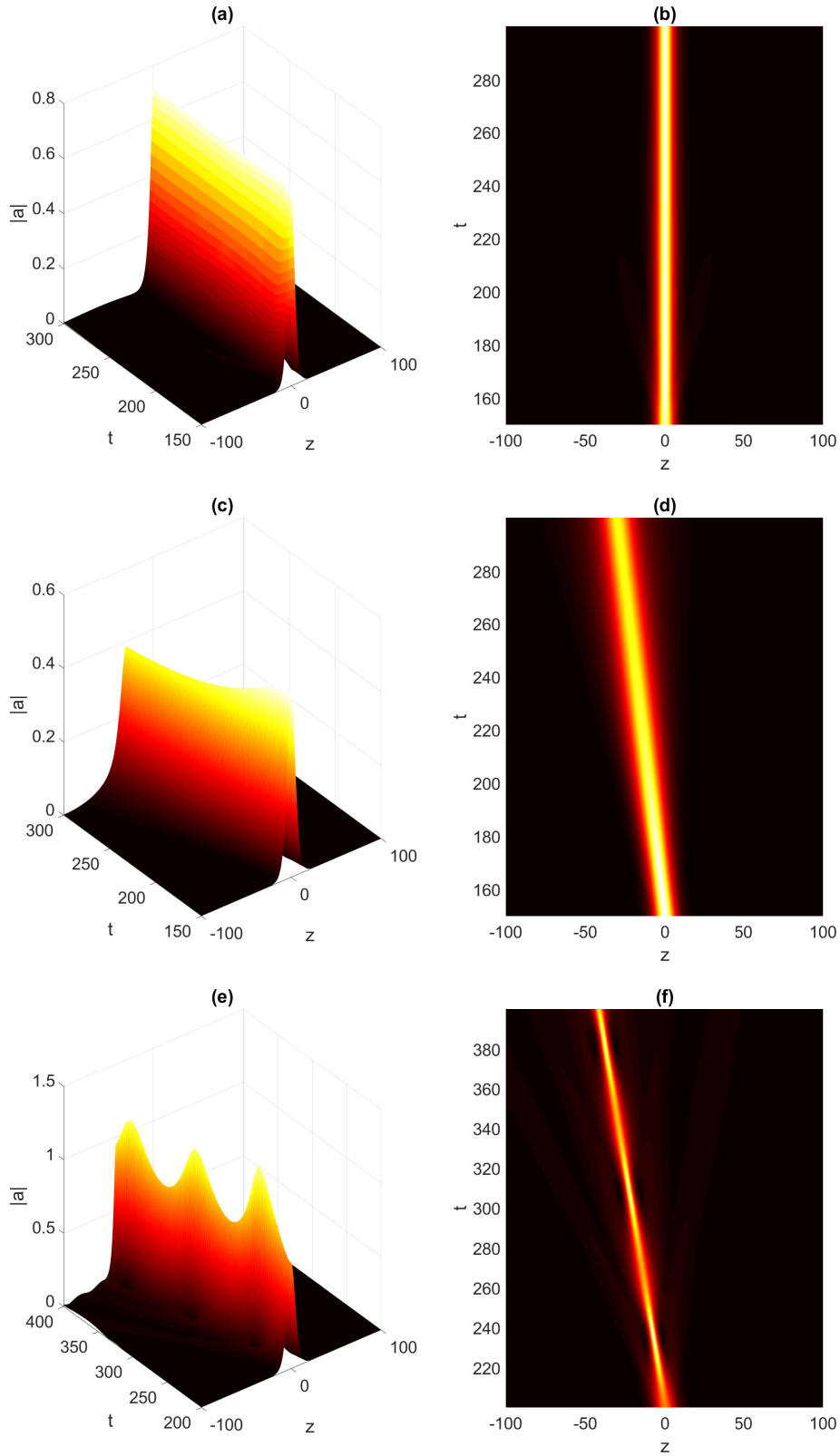


FIG. 4. Spatio-temporal evolution of the generalized nonlinear Schrödinger (GNLS) equation (11) in different dynamical regimes for a fixed value of the degeneracy parameter $R_0 = 0.02$. Left panels are the surface plots of soliton solutions, while the right panels represent the corresponding contour plots. Subplots (a) and (b) show an evolution of standing soliton in the stable region with soliton velocity $v_0 = 0$, the soliton eigenfrequency $\lambda = 0.207$, the amplitude $a_0 = 0.68$ and the soliton photon number $P_0 = 1.46$; Subplots (c) and (d) a moving soliton in the stable region with an increasing velocity $v_0 = 0.2$, the same $\lambda = 0.207$ but different $a_0 = 0.67$ and $P_0 = 1.12$; Subplots (e) and (f) a moving soliton in the stable region with the same $v_0 = 0.2$ as in [(c) & (d)] but different $a_0 = 0.72$, $\lambda = 0.26$ and $P_0 = 1.55$.

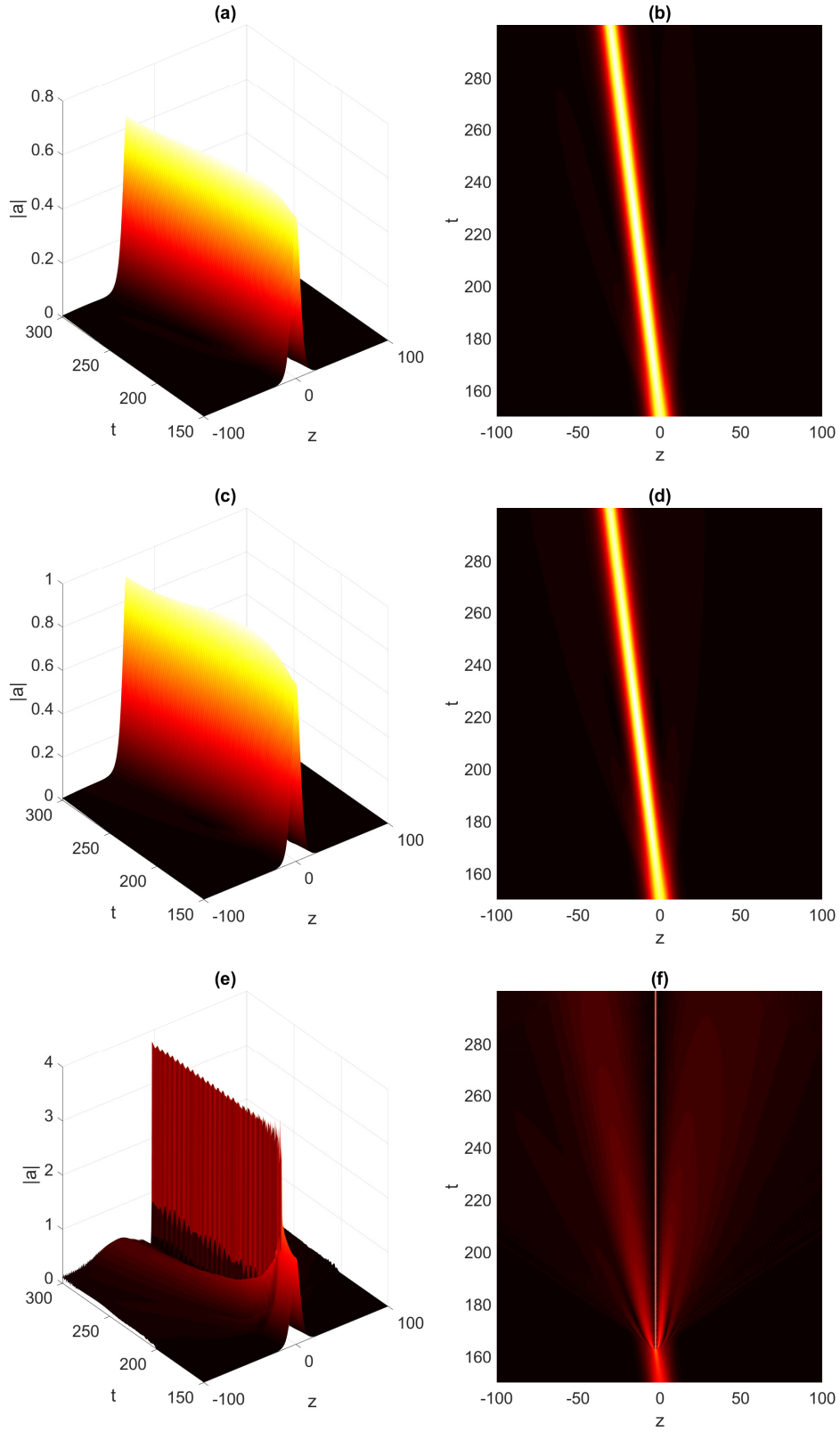


FIG. 5. Spatio-temporal evolution of the generalized nonlinear Schrödinger (GNLS) equation (11) for different values of the degeneracy parameter R_0 : $R_0 = 0.02$ in the stable region [subplots (a) and (b)], $R_0 = 0.8$ in the stable region [subplots (c) and (d)], and $R_0 = 2$ in the unstable region [subplots (e) and (f)]. The other parameter values are fixed at $v_0 = 0.2$ and $\lambda = 0.23$.

due to nonlinear interactions of linearly polarized intense laser light and relativistic degenerate dense plasmas in the framework of the generalized nonlinear Schrödinger (GNLS) equation with local and nonlocal nonlinearities. The latter appear due to the laser driven ponderomotive force, and the generation of odd and even harmonics for the vector potential and the electron density perturbation respectively. An analytical moving soliton solution of the GNLS equation and the corresponding soliton photon number P are derived each in a closed form.

A linear stability analysis of the soliton solution is performed according to the Vakhitov-Kolokolov stability criteria. Different stable and unstable regions are demonstrated in the plane of the soliton velocity v_0 and the eigenfrequency λ for different values of the degeneracy parameter R_0 . It is found that the stability region shifts to an unstable one and is significantly reduced as R_0 increases from the regimes of weak to strong relativistic degeneracy. However, both the stable and unstable regions get significantly shrunk when $R_0 \gg 1$, i.e., in the limit of ultrarelativistic degeneracy, and eventually no feasible region can be found. This may be the limitation of the Vakhitov-Kolokolov stability criteria which may not predict the stability region for $R_0 \gg 1$. The stability analysis shows that the moving EM solitons in the weakly relativistic regime are stable with the stability region shifting towards smaller amplitudes in comparison with the standing soliton. However, as one enters from the weak to strong degenerate regime, the perturbation grows, i.e., the soliton stability region shifts towards larger amplitudes, and eventually the soliton collapses at higher value of $R_0 > 1$. Furthermore, it is found that for an isolated soliton with a constant photon number, an increase of the soliton velocity results into a reduction of the maximum amplitude and broadening of the soliton profile. Numerical simulation results of the GNLS equation are found to be in good agreement with our analytical predictions for the existence and stability of EM solitons.

It is to be noted that the determination of different dynamical regimes of EM solitons in the parameter space (P, λ) discussed above is important for understanding the low-frequency process of the formation of stable relativistic solitons behind the laser pulse inside the photon condensate [14]. However, the detailed analysis of the regions in the parameter space requires additional analytical and numerical study which is beyond the scope of the present work.

To conclude, the results should be useful for understanding the interactions of linearly polarized highly intense laser pulses with relativistic degenerate dense plasmas and their experimental verification as such experiments are going on with new generation of intense lasers, as well as the characteristics of x-ray pulses emanating from compact astrophysical objects.

ACKNOWLEDGMENTS

This work was supported by the Science and Engineering Research Board (SERB), Govt. of India with Sanction order no. CRG/2018/004475 dated 26 March 2019.

DATA AVAILABILITY STATEMENTS

Data sharing is not applicable to this article as no new data were created or analyzed in this study.

Appendix A

Here, we give some details of the derivation of the GNLS equation (11).

We consider the perturbation expansions for A and N as

$$\begin{aligned} A &= \frac{1}{2} (ae^{-it} + a^*e^{it}), \\ N &= N_0 + \frac{1}{2} (N_2e^{-i2t} + N_2^*e^{i2t}). \end{aligned} \quad (\text{A1})$$

Substituting Eq. (A1) into Eq. (8) we get

$$\begin{aligned} &\left(\frac{\partial^2}{\partial t^2} - \delta_e \frac{\partial^2}{\partial z^2} + 1 \right) \left(N_0 + \frac{1}{2} N_2 e^{-i2t} + \frac{1}{2} N_2^* e^{i2t} \right) \\ &= \frac{1}{2} (1 - \delta_e) \frac{\partial^2}{\partial z^2} \left[\frac{1}{2} (ae^{-it} + a^*e^{it}) \right]^2, \end{aligned} \quad (\text{A2})$$

or,

$$\begin{aligned} &-2N_2e^{-i2t} - 2N_2^*e^{i2t} + N_0 + \frac{1}{2}N_2e^{-i2t} + \frac{1}{2}N_2^*e^{i2t} \\ &= \frac{1}{8}(1 - \delta_e) [(a^2)_{zz}e^{-i2t} + 2(|a|^2)_{zz} + (a^{*2})_{zz}e^{i2t}] \end{aligned} \quad (\text{A3})$$

Collecting the zeroth and second harmonic terms ($\sim e^{-i2t}$), which appear due to self-interactions of waves, from both sides of Eq. (A3), we obtain the following expressions for N_0 and N_2 .

$$\begin{aligned} N_0 &= \frac{1}{4}(1 - \delta_e)(|a|^2)_{zz}, \\ N_2 &= -\frac{1}{12}(1 - \delta_e)(a^2)_{zz}. \end{aligned} \quad (\text{A4})$$

Next, substituting Eq. (A1) into the wave equation (7) and using Eq. (A4) we obtain

$$\begin{aligned} &\left(\frac{\partial^2}{\partial t^2} - \frac{\partial^2}{\partial z^2} + 1 \right) \left[\frac{1}{2} (ae^{-it} + a^*e^{it}) \right] \\ &+ (1 - \delta_e) \left[N_0 + \frac{1}{2} (N_2e^{-i2t} + N_2^*e^{i2t}) \right] \\ &- a \left(\frac{1}{2} (ae^{-it} + a^*e^{it}) \right)^2 \frac{1}{2} (ae^{-it} + a^*e^{it}) = 0, \end{aligned} \quad (\text{A5})$$

or,

$$\begin{aligned}
& \frac{1}{2} \frac{\partial^2 a}{\partial t^2} e^{-it} - i \frac{\partial a}{\partial t} e^{-it} - \frac{1}{2} a e^{-it} + \frac{1}{2} \frac{\partial^2 a^*}{\partial t^2} e^{it} + i \frac{\partial a^*}{\partial t} e^{it} \\
& - \frac{1}{2} a^* e^{it} - \frac{1}{2} (a)_{zz} e^{-it} - \frac{1}{2} (a^*)_{zz} e^{it} \\
& + \frac{1}{2} a e^{-it} + \frac{1}{2} a^* e^{it} + \left[\frac{1}{4} (1 - \delta_e)^2 (|a|^2)_{zz} - \frac{1}{24} (1 - \delta_e)^2 (a^2)_{zz} e^{-i2t} \right. \\
& \left. - \frac{1}{24} (1 - \delta_e)^2 (a^{*2})_{zz} e^{i2t} \right] \frac{1}{2} (a e^{-it} + a^* e^{it}) = 0
\end{aligned} \tag{A6}$$

sides of Eq. (A6) we get

$$\begin{aligned}
& \frac{1}{2} \frac{\partial^2 a}{\partial t^2} - i \frac{\partial a}{\partial t} - \frac{1}{2} a - \frac{1}{2} (a)_{zz} + \frac{1}{2} a \\
& + \frac{1}{8} (1 - \delta_e)^2 (|a|^2)_{zz} a - \frac{1}{48} (1 - \delta_e)^2 (a^2)_{zz} a^* \\
& - \frac{1}{8} \alpha (1 - \delta_e) a^2 a^* - \frac{1}{4} \alpha (1 - \delta_e) |a|^2 a = 0.
\end{aligned} \tag{A7}$$

For slowly varying wave envelopes, the terms involving $\partial^2/\partial t^2$ ($\ll 1$) may be neglected. Finally, we obtain from Eq. (A7) the following wave equation for a .

$$\begin{aligned}
& i \frac{\partial a}{\partial t} + \frac{1}{2} (a)_{zz} + \frac{3}{8} \alpha (1 - \delta_e) |a|^2 a - \frac{1}{8} (1 - \delta_e)^2 (|a|^2)_{zz} a \\
& + \frac{1}{48} (1 - \delta_e)^2 (a^2)_{zz} a^* = 0.
\end{aligned} \tag{A8}$$

Collecting the first harmonic terms ($\sim e^{-it}$) from both

-
- [1] A. P. Misra, and S. Banerjee, Phys. Rev. E **83**, 037401 (2011).
- [2] G. O. Williams, H.-K. Chung, S. Künzel, V. Hilbert, U. Zastra, H. Scott, S. Daboussi, B. Iwan, A. I. Gonzalez, W. Boutu *et al.*, Phys. Rev. Research **1**, 033216 (2019).
- [3] A. C. Hayes, M. E. Gooden, E. Henry, G. Jungman, J. B. Wilhelmy, R. S. Rundberg, C. Yeamans, G. Kyrala, C. Cerjan, D. L. Danielson *et al.*, Nat. Phys. **16**, 432 (2020).
- [4] T. M. Jeong and J. Lee “Generation of High-Intensity Laser Pulses and their Applications” DOI: 10.5772/64526.
- [5] F. Verheest, Phys. Scr. **90**, 068002 (2015).
- [6] F. Verheest, Phys. Scr. **91**, 025603 (2016).
- [7] I. Bersons, R. Veilande, and O. Balcers, Phys. Scr. **95**, 025203 (2020).
- [8] A. R. Holkundkar and G. Brodin, Phys. Rev. E **97**, 043204 (2018).
- [9] G. Lehmann, E. W. Laedke, and K. H. Spatschek **13**, 092302 (2006).
- [10] S. Sundar, A. Das, V. Saxena, P. Kaw, and A. Sen, Phys. Plasmas **18**, 112112 (2011).
- [11] G. Mikaberidze and V. I. Berezhniana, Phys. Lett. A **379**, 2730 (2015).
- [12] V. I. Berezhniana, N. L. Shatashvili, and N. L. Tsintsadze, Phys. Scr **90**, 068005 (2015).
- [13] A. Mancic, L. Hadzievski, and M. M. Skoric, Phys. Plasmas **13**, 052309 (2006).
- [14] Lj. Hadzievski, M. S. Jovanovic, M. M. Skoric, and K. Mima, Phys. Plasmas **9**, 2569 (2002).
- [15] S. Roy, D. Chatterjee, and A. P. Misra, Phys. Scr. **95**, 015603 (2020).
- [16] F. T. Gratton, G. Gnani, R. M. O. Galvao, and L. Gomberoff, Phys. Rev. E **55**, 3381 (1997).
- [17] A. P. Misra and D. Chatterjee, Phys. Plasmas **25**, 062116 (2018).
- [18] S. Chandrasekhar, Mon. Not. R. Astron. Soc. **95**, 207 (1935).
- [19] N. G. Vakhitov and A. A. Kolokolov, Izv. Vyssh. Uchebn. Zaved. Radiofizika **16**, 1020 (1973).
- [20] A. G. Litvak and A. M. Sergeev, JETP Lett. **27**, 517 (1978).
- [21] E. Pelinovsky, V. V. Afanasijev, and Y. S. Kivshar, Phys. Rev. E **53**, 1940 (1996).